Design of a Haptic Feedback System for Flight Envelope Protection

Van Baelen, Dirk; Ellerbroek, Joost; van Paassen, Rene; Mulder, Max

DOI
10.2514/1.G004596

Publication date
2020

Document Version
Final published version

Published in
Journal of Guidance, Control, and Dynamics: devoted to the technology of dynamics and control

Citation (APA)
Van Baelen, D., Ellerbroek, J., van Paassen, R., & Mulder, M. (2020). Design of a Haptic Feedback System for Flight Envelope Protection. *Journal of Guidance, Control, and Dynamics: devoted to the technology of dynamics and control*, *43*(4), 700-714. https://doi.org/10.2514/1.G004596

JOURNAL OF GUIDANCE, CONTROL, AND DYNAMICS
Vol. 43, No. 4, April 2020

Design of a Haptic Feedback System for Flight Envelope Protection

Dirk Van Baelen,* Joost Ellerbroek,† M. M. (René) van Paassen,‡ and Max Mulder§
Delft University of Technology, 2629 HS Delft, The Netherlands

https://doi.org/10.2514/1.G004596

Several modern aircraft use a passive control manipulator: a spring–damper system that generates command signals to the flight control computers in combination with a flight envelope protection system that limits pilot inputs when approaching the aircraft limits. This research project aims to increase pilot awareness of this protection system through the use of force feedback on the control device, that is, haptics. This paper describes in detail how the haptic feedback works and when it triggers; another paper will discuss the results of an experimental evaluation. With the current haptic design, pilots can get five cues: first, a discrete force cue when approaching the limits; second, an increased spring coefficient for control deflections that bring the aircraft closer to its limits; third, a stick shaker for low velocities; fourth, if a low-velocity condition requires an input, the stick is moved forward to the desired control input; and finally, the stick follows the automatic Airbus "pitch-up" command during an overspeed condition. This novel system is expected to help pilots correctly assess the situation and decide upon the right control action. It will be evaluated in two scenarios close to the flight envelope limits: a windshear and an icing event.

Nomenclature

a	=	acceleration, m/s^2
C_L	=	lift coefficient
D	=	drag, N
F	=	force, N
g	=	gravitational acceleration, m/s^2
K	=	gain
k	=	spring, N/rad
L	=	lift, N
m	=	mass, kg
n	=	load factor, g
q	=	pitch rate, rad/s
S	=	surface, m^2
T	=	thrust, N
t	=	time, s
V	=	velocity, m/s
W	=	weight, N
α	=	angle of attack, rad
β	=	sideslip angle, rad
γ	=	flight path angle, rad
δ	=	control device deflection, rad
θ	=	pitch angle, rad
ρ	=	density, kg/m^3
φ	=	roll angle, rad

Subscripts

br	=	breakout
max	=	maximum value
min	=	minimum value
nom	=	nominal value
np	=	neutral point
prot	=	protected region value

Presented as Paper 2018-0117 at the 2018 AIAA Modeling and Simulation Technologies Conference, Kissimmee, FL, 8–12 January 2018; received 29 May 2019; revision received 30 October 2019; accepted for publication 5 November 2019; published online 28 February 2020.

*Ph.D. Student, Control and Simulation, Kluyverweg 1; d.vanbaelen@tudelft.nl. Student Member AIAA.

†Assistant Professor, Control and Simulation, Kluyverweg 1; j.ellerbroek@tudelft.nl.

‡Associate Professor, Control and Simulation, Kluyverweg 1; m.m.vanpaassen@tudelft.nl.

§Professor, Control and Simulation, Kluyverweg 1; m.mulder@tudelft.nl. Associate Fellow AIAA.

I. Introduction

MODERN cockpits provide an abundance of information to pilots, primarily using the visual and auditory communication channels. Examples of visual displays are the primary flight display (PFD) for the most important aircraft states and the navigation display for a planar top-down overview of the environment. Auditory signals are often used to provide urgent messages, such as to warn pilots for too high velocities and to provide altitude readouts and throttle back commands on landing [1].

But, apart from these senses, pilots are able to perceive information in several other ways. This paper will elaborate on the use of the pilot's haptic sense by providing haptic feedback through the control device. As shown in Fig. 1, within the field of haptic research, two main categories are identified: touch (stimuli to the skin) and kinaesthesis (stimuli to the receptors in the muscles, joints, and tendons) [2,3]. The design discussed in this paper uses both touch and kinaesthesis; hence, the term haptic feedback is used.

In classical aircraft, the control manipulator "feel" provided information on, for instance, aerodynamic forces, buffeting when close to a stall, actuator saturation through hard stops of the controls, and other control-related phenomena. With the introduction of fly-by-wire, however, the forces on the control surfaces and the control devices were decoupled, eliminating this potentially very useful haptic information channel [4].

A reason that haptic feedback was not integrated after the introduction of fly-by-wire systems in the 1980s and 1990s was the rather bulky device required to implement the haptic forces. Whereas these old devices had issues regarding their size, weight, power, and stability requirements, current-day devices have become much smaller and lighter while still being able to provide reliable haptic feedback [5]. This offers the possibility to reconsider this type of feedback in fly-by-wire control systems [6].

Together with the advances in control devices, automation in cockpits is rising, resulting in a more supervisory role for the pilot instead of direct manual control. Despite these advances, pilots are still often required to take over manual control of the aircraft in landing, takeoff, or during emergency scenarios. An example of the latter could be a computer or sensor malfunction, which was the case for Air France flight 447 [7]. The crew, startled by unexpected high-altitude dynamics, lost situation awareness despite the information available from the visual and aural displays. Unaware of the loss of the usual flight envelope protections due to the malfunction,

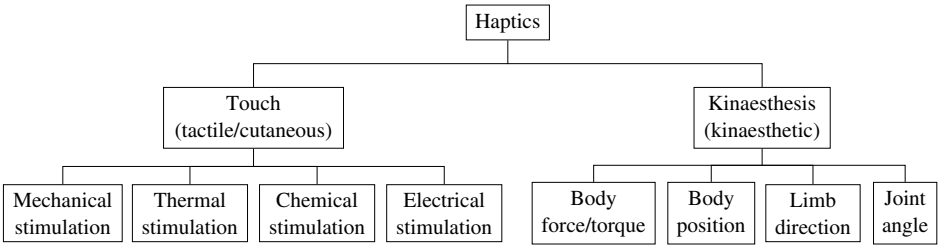

Fig. 1 Components of haptics [3].

pilots stalled the aircraft. The control manipulator, which was the Airbus A330 sidestick, provided the pilots with neither direct feedback on their control actions nor the aerodynamic stall buffets; i.e., it did not help them in properly identifying the situation as a stall. As this tragic example shows, when manual control is needed, the lack of haptic information through the control device might contribute to a reduced situation awareness.

Combining the ever-increasing sophistication of automation on the flight deck and the current generation of small and powerful control devices provides designers a new opportunity, namely, to increase pilot awareness through haptic feedback. Some aircraft already include "augmented forces" on the control device, which can be provided on both control devices (in a two-pilot cockpit) linked to the surfaces or fly-by-wire control systems. An example of this is the "Q-feel force," which changes the stiffness of the controls with changing dynamic pressure/velocity in Boeing-type aircraft [8]. Another example is a stick shaker or pusher, which warns pilots of moving closer to extreme aircraft states [9]. The control device can also be loaded with two passive springs to create a change in spring coefficient when pilots exert large control deflections, irrespective of the aircraft state, such as done in Airbus aircraft. Active control can be used to have an increased (artificial) spring force when rolling beyond the safe roll limit, irrespective of the control surfaces, as used in a Boeing 777 [10].

Although examples of haptic feedback implementations exist, there is limited research published in the open literature to prove the benefits of such a system. Within the field of aerospace, one example uses a passive spring or an active counterforce to communicate the distance to the flight envelope limits. The latter gave the best tracking performance increase as compared to the baseline condition [11]. A second example is the work by Stepanyan et al. that showed the limit on the available control space both visually and haptically [12]. For the haptics, they changed the input neutral point and the maximum deflection, which was used by the pilots to operate the aircraft at the limits. A soft stop (i.e., a local step in the force required for a certain deflection) can be used to indicate the engine limitations in the collective of a helicopter. It was shown in simulations that such a system can reduce the workload of the pilot [13,14]; this was implemented in an experimental helicopter of the DLR, German Aerospace Center [15]. Tactile feedback through the use of vibrating elements on a vest, i.e. tactors, enabled spatial awareness and reduced spatial disorientation [16]. These examples use haptic feedback to inform the pilot about the flight envelope limits. Note that research in supplying the pilot with such information is not limited to haptic only; new visual displays are investigated as well and show positive results [17]. Aside from information on the flight envelope limits, the haptic channel can additionally be used to supply guidance support, of which a haptic flight director showed great potential to increase the pilot tracking error and reduce workload [18]. Other fields do show a larger public research interest in this domain, for example, in teleoperation: the control of an unmanned vehicle was supported by haptically showing the proximity to objects in its surroundings. It resulted in decreased workload and increased situation awareness for the given navigation task [19]. In the automotive field, haptics can be used on the gas pedal to show the proximity of a car in front, resulting in an increased performance while reducing input magnitudes [20]. Haptics can additionally be used to support curve negotiation through the steering wheel using two approaches: i) warning systems which reduce the reaction time of the driver while have a potential to induce driver-annoyance, and ii) guidance systems (for example to the center of the road) improved performance yet are subjective to after-effects [21].

The aim of the current project is to investigate the use of haptic feedback to give the pilot more information on the augmentation with respect to the limits of the aircraft during manual control within the modern fly-by-wire cockpit. In other words, the design presented in the following aims to provide feedback to the pilot on the proximity of the state to the flight envelope limits. Only longitudinal haptic feedback is considered here; lateral cues can be added in a future design using the same design ideas. This work builds on an initial study [22], which already showed a potential benefit of such a haptic feedback system. The goal of this paper is to elaborate on a new iteration and give a thorough description on the how and when of the haptics, as well as the expected practical implications.

Section II will first discuss some basic flight dynamics and will introduce the control laws and flight envelope protection system present in current fly-by-wire Airbus aircraft. Section III discusses the rationale of our haptic interface, which is designed to present some of the functions of these automated systems. We then discuss two operational scenarios where the flight envelope protection system will trigger (a windshear and an icing event) to explain in detail how our haptic interface works (Sec. IV). Finally, conclusions are given in Sec. V.

II. Flight Dynamics and Control Laws

This section provides the background needed to understand the design rationale of our haptic interface. Section II.A covers some basic flight dynamics properties and variables. Readers familiar with aircraft flight dynamics can skip this subsection. Because our haptic design focuses on supporting pilots in working with the complex Airbus control law and flight envelope protection structures, a brief recap of these structures is provided in Sec. II.B. This recap only discusses the (highly coupled) protections; yet, the level of detail is sufficient to support the design of the haptic feedback system in the following.

A. Flight Dynamics

This subsection explains a basic set of flight dynamics variables that is essential to understand the aircraft control laws and the application of the haptics. A full discussion on flight dynamics can be found in the literature [23]. The bank angle ϕ, indicating how much the aircraft wing is tilted with respect to the horizontal plane, is the most important lateral variable and is depicted in Fig. 2a. The relevant longitudinal angles are shown in Fig. 2b: the pitch angle θ depicts the angle of the nose of the airplane relative to the horizon, the flight path angle γ gives the elevation of the true velocity vector V with respect to the horizon, and the angle of attack α is the angle of incidence of the air with the wing section. Accelerations are expressed in the aircraft body reference frame; the vertical acceleration a_z is commonly expressed in the load factor ($n = (a_z/g)$) and is shown in Fig. 2b. Typical level cruise flight is performed with a load factor of one: the lift is equal to the weight. By pitching up, the load factor is increased, which is experienced as "being pushed in the seat," and vice versa.

Limits of the aircraft are typically expressed in a flight envelope (FE). Different combinations of variables are possible; yet, as Airbus control laws are mostly load factor dependent, this research considers only the relation between the aircraft velocity V and the load factor n.

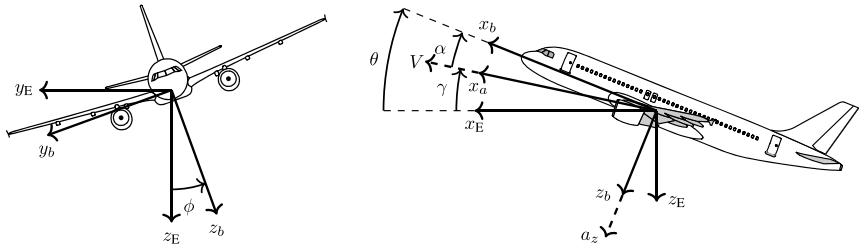

a) View from the front **b) View from the left**

Fig. 2 A320 model used in the research with the most important angles indicated (all positive).

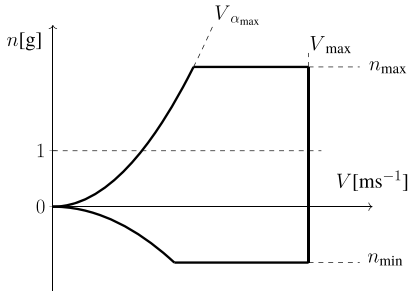

Fig. 3 Flight envelope: allowable load factor n versus allowable velocity V.

This The FE is depicted by the solid black line in Fig. 3. The upper velocity limit (right-hand vertical line) is due to the maximum velocity V_{max} created by aerodynamic and vibration limits. Extreme load factor values are determined by static structural limits and indicated by the upper n_{max} and lower n_{min} horizontal lines. The lower velocity limits $V_{\alpha_{max}}$ (the left-hand side of Fig. 3) follow a quadratic relation with velocity due to the lift equation shown in Eq. (1), where ρ is the density of the air, S is the lifting surface of the wing, and C_L is the lift coefficient:

$$L = \frac{1}{2}\rho V^2 S C_L \tag{1}$$

The latter coefficient C_L depends on the wing shape and on the angle of attack: the higher the α, the higher the lift coefficient, up to a maximum value α_{max}, where this coefficient suddenly drops and a stall occurs.

B. Airbus Control Laws

To better understand when the haptic feedback is applied, it is important to understand how the pilot controls the aircraft. As this research focuses on an Airbus A320, the main control device used is discussed: the sidestick. All information in the following is retrieved from the A320 Flight Crew Operation Manual (FCOM) [24].

The Airbus sidestick is a passively loaded control device: the "stick feel" is provided by springs and dampers. The device is not mechanically coupled to the control surfaces (ailerons, elevator); it produces an electrical signal to the flight control computers (FCCs), as shown in Fig. 4. The latter are responsible for converting the sidestick deflections to required control inputs and combining them with the autopilot control commands to control surface deflections. As such, the FCCs can override the pilot inputs and, in doing that, provide an additional layer of safety to keep the aircraft states inside the allowed FE region. This process is called flight envelope protection (FEP) and is applied for both lateral and longitudinal inputs, as will be elaborated on in the following.

The FCCs consist of seven computers with three functions: i) two elevator and aileron computers (ELACs) for elevator and stabilizer control, and constant aileron control; ii) three spoilers and elevator computers (SECs) for spoilers control and standby elevator and stabilizer control; iii) two flight augmentation computers (FACs) for electrical rudder control. These computers are provided with information on the aircraft states by a number of systems and sensors: 1) air data and inertial reference unit, 2) slat flap control computer (SFCC), 3) accelerometers, 4) landing gear control interface unit (LGCIU), 5) radio altimeter (RA), and 6) flight management guidance computer.

Five control laws with different levels of support are possible within the Airbus philosophy. This paper will not discuss in detail when each of the control laws is active. The selection of control law is based on internal sensor validity checks, for which more details can be found in the FCOM (Ref. [24]). Only a general description, together with the control laws, follows. We start with the "normal law," which provides the most assistance to pilots, and then we move to the configurations that provide less assistance ("alternate control law with reduced protections" and "alternate control law without reduced protections"). The "direct law" and "mechanical backup" are included for the sake of completeness but will not be used in the sections that follow. A summary of the control laws can be found in Table 1, and all the protections are in Table 2.

1. *Normal Control Law*

When all systems are functioning nominally, the FCCs operate in the normal control law (NL), which is the default control mode. The pilot longitudinal and lateral control inputs are both interpreted as "reference" signals for the FCCs, as will be discussed in the following. In addition, the FEP applies a number of protections to prevent the aircraft from moving outside the, what is considered safe, flight envelope. Examples are the bank angle limitation, the load factor limitation, the pitch attitude protection, the high angle-of-attack protection, and the high-speed protection.

a. Lateral Control. The FCC interprets lateral stick deflections as commands to change the bank angle. From 0 to 33 deg of bank, the sidestick lateral deflection is a bank angle rate command, whereas the

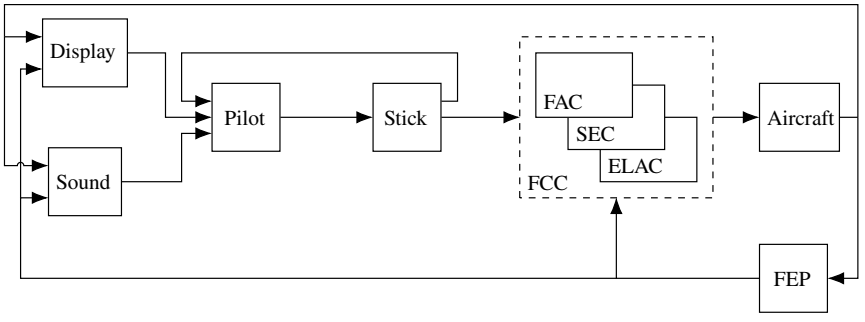

Fig. 4 Block diagram representing the Airbus control loop.

bank from 33 deg up to 67 deg is a bank angle command. The maximum bank angle rate achievable with full deflection is 15 deg/s. The FEP in the FCCs limits the maximum achievable bank to 67 deg, which is the first hard envelope limit. If the bank angle exceeds 33 deg, positive bank stability is present such that the aircraft automatically rolls back to 33 deg when the sidestick is not deflected. Hence, in case the pilot intends to execute a steep turn, a constant stick deflection is required. To assist the pilot during horizontal turns, for bank angles up to 33 deg, an automatic pitch command is added such that the pilot does not need to maintain backpressure on the stick to compensate for the required increase in lift.

Additionally, the autopilot disconnects when the bank angle exceeds 45 deg; at which point, the flight director (FD) bars (indication of the guidance by the FCC on the PFD) disappear. The bars return when the bank angle reduces below 40 deg. To prevent excessive trimmable horizontal stabilizer (THS) deflections due to the manual or autotrim functionality, the deflection is limited between the value on entering of the protection and 3.5 deg nose-down. Finally, limits for the bank angle depend on the longitudinal protections, which are elaborated on in the following. A visual summary of the lateral protections can be found in Fig. 5 [24].

Table 1 Summary of airbus flight control laws

Direction	Normal law	Alternate law
Lateral	1) Bank rate demand	1) Bank direct stick-to-surface
	2) 15 deg/s for full lateral deflection	2) Clean maximum of 30 deg/s
		3) Otherwise, 25 deg/s
Longitudinal	1) C^* control law	Control law equal to NL
	2) Autotrim for changing speed or configuration	
	3) Automatic pitch compensation for $\phi \leq \pm 33$	

Table 2 Summary of airbus flight envelope protection

Variable	Normal law	Alternate law
Bank ϕ	THS limited between entry value and 3.5 deg nose-down	Autopilot disconnects when $\phi > 45$ deg
	Autopilot disconnects when $\phi > 45$ deg	No other protections
	FD bars disappear when $\phi > 45$ deg	
	FD bars return when $\phi < 40$ deg	
	Nominal maximum: 67 deg	
	Maximum with α_{prot} active: 45 deg	
	Maximum with $V > V_{MO}$: 40 deg	
	Nominal protection: positive bank stability to ± 33 deg	
	Protection with $V > V_{MO}$: positive bank stability to 0 deg	
Pitch θ	No limit for Autopilot	— —
	Nose-up maximum, flaps 0–3: 30 deg	
	Nose-up maximum, full flaps: 25 deg	
	Nose-down maximum: -15 deg	
	FD bars disappear when $\theta > 25$ deg or $\theta < -13$ deg	
	FD bars return when $\theta < 22$ deg or $\theta > -10$ deg	
High angle of attack α	THS limited between entry value and 3.5 deg nose-down	— —
	Autopilot disconnects when $\alpha > \alpha_{prot}$	
	Pilot input proportional in region: $\alpha_{prot} \rightarrow \alpha_{max}$	
	Protection deactivates: when 8 deg forward input or 0.5 deg forward for 0.5 s when $\alpha < \alpha_{max}$	
	Below 200 ft, protection deactivates when pilot input half of nose-up input or when $\alpha < \alpha_{prot} - 2$	
	When $\alpha > \alpha_{floor}$, thrust is set to takeoff/go-around[a]	
Low velocity V	— —	At 5–10 KTS above V_{SW}[b]: a nose-down command is inserted with bank angle compensation to keep α constant
		An aural "STALL" warning is provided with appropriate margin from stall
High velocity V	THS limited between entry value and 11 deg nose-up	When $V > V_{max}$: autopilot disconnects
	When $V > V_{max}$[c]: autopilot disconnects	Nose-up command is inserted
	pilot nose-down authority is reduced	and can be overruled by pilot
	an automatic nose-up command is introduced	When $V > V_{MO} + 4$:
	command cannot be overruled by pilot	an aural "Overspeed" warning sounds
Load factor n_z	THS limited between entry value and 3.5 deg nose-down when $n > 1.25$	Equal to normal law
	Maximum, clean: 2.5	
	Maximum, with flaps/slats: 2	
	Minimum, clean: -1	
	Minimum, with flaps/slats: 0	

[a]$\alpha_{floor} = 9.5$ deg without flaps/slats (15 deg for configurations 1 and 2, 14 deg for configuration 3, and 13 deg for full) or when pilot inputs 14 deg pitch-up with either pitch or angle-of-attack protection active.

[b]Speed margin according to Airbus documentation: "Based on the aircraft gross weight and slats/flaps configuration."

[c]Airbus documentation is unclear on the exact activation point: "at/or above V_{max}."

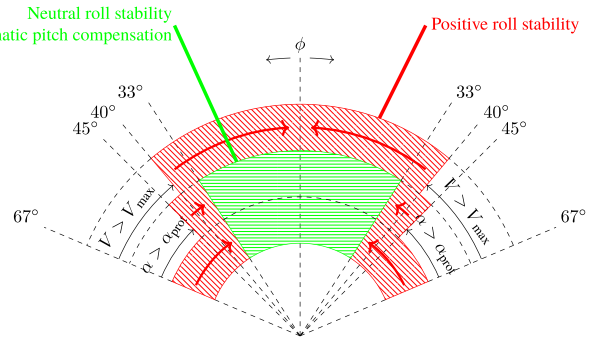

Fig. 5 Lateral control in NL, based on the A320 FCOM [24].

b. Longitudinal Control. For longitudinal control, Airbus uses the C^* approach, which is a combination of both the pitch rate q and the load factor n [24–27]. In the low-speed regime, up to approximately 240 kt, the pilot stick deflections are interpreted as pitch rate commands; in high-speed regions, the stick deflections are interpreted as load factor commands [27]. Due to this setup, there is no need for the pilot to trim the aircraft for changing velocity or configuration.

On top of the C^* control law, protections are present on the pitch angle, the angle of attack, the load factor, and high velocities. The limit on the pitch angle and load factor is without any buffer zone: when approaching the limit, the FCC gradually reduces the pitch rate/load factor until the maximum value is reached and no further control can be achieved. For the other limit, which is the angle of attack, there is a zone from a protected value α_{prot} up to the maximum value α_{max} where the C^* control law is altered to provide position control from the control device deflection, which is proportional to the angle of attack approaching the limit. Additionally, the autopilot disconnects when entering the protected region, and the maximum achievable bank is reduced to 45 deg to prevent asymmetric stall. The throttle input is automatically set to takeoff/go-around setting when the angle of attack increases beyond α_{floor} (9.5 deg without flaps/slats, 15 deg for configurations 1 and 2, 14 deg for configuration 3, and 13 deg for full) or the control device deflection is larger than 14 deg nose-up with pitch or angle-of-attack protection active.

The angle-of-attack protection deactivates when the pilot pushes the control device more than 8 deg forward, or when (s)he pushes at least 0.5 s with a deflection of a minimal of 0.5 deg forward when the angle attack is below the maximum value. Below 200 ft, the protection is also deactivated by using less than half of the nose-up input or when the angle of attack is less than $\alpha_{prot} - 2$ deg.

For all three limits, the maximum value (and, if applicable, the size of the position control zone) depends on the particular flight conditions and the state of the aircraft. The pitch angle limits are between −15 and 30 deg (25 deg for full flaps/slats); the load factor must remain between −1 and 2.5g without flaps/slats (0 and 2g for any other configuration); and the angle of attack must remain less than 12 deg, with a protection zone of 2 deg. The buffer zone for the angle of attack is shown on the PFD through the velocity indication, whereas no indication for the load factor is available in the current Airbus setup; hence, this could be useful extra information to the pilot. Note that the pitch limits do not apply to the autopilot and that the FD bars disappear when the pitch increases above 25 deg nose-up or below 13 deg nose-down, and they return when the pitch is between 22 deg nose-up and 10 deg nose-down.

To prevent structural damage when controlling the aircraft at high velocities, a high-speed protection is present. This protection triggers at the maximum operational velocity (V_{max} or above, depending on the configuration), disconnects the autopilot, and activates an automatic nose-up command while reducing the nose-down stick authority to reduce the airspeed below the maximum, effectively creating an artificial high-speed stability. The pilot is warned of the overspeed condition by an aural message, yet the nose-up command is not communicated to the pilot. Enabling the pilot to know (or feel) how it is implemented can be an addition. Note that the nose-up command cannot be overridden by the input of the pilot: even with full forward deflection. To avoid abnormal attitudes during this situation, the positive bank stability shown in Fig. 5 rolls the aircraft back to 0 deg; and the maximum bank angle is limited to 40 deg. These additional limitations are present until the velocity drops below the maximum velocity.

As for the lateral control, here, the THS is limited to prevent excessive deflections. During the angle-of-attack protection and load factor values above 1.25g, the limits are the entry value and 3.5 deg nose-down. When the high-velocity protection is active, maximum values are the entry value and 11 deg nose-up.

Figure 3 already showed the nominal flight envelope. Here, we discuss the angle of attack [related to velocity through Eq. (1)], the load factor, and high-velocity protections present in the A320 control laws. The angle-of-attack protection can be visualized on the flight envelope, as shown with the red dashed line on Fig. 6, where every state where no protection is active is defined as belonging to the safe flight envelope (SFE). As can be seen in the figure, the zone where a protection is active provides a buffer for the pilot when approaching the limits.

2. *Alternate Control Law with Reduced Velocity Protections*

In case of sensor or computer failures, the FCC reverts back to control laws that provide less support for the pilot. The first of these degraded control laws is the alternate control law (AL), with reduced protections, which triggers when a dual failure of the computers are present.

a. Lateral Control. Lateral control becomes a direct stick-to-control-surface-position relationship with maximum bank rate of 30 deg/s for the clean configuration and 25 deg/s otherwise. Hence, the positive bank stability and the bank angle protection are lost. Furthermore, if the autopilot is engaged, it disconnects at 45 deg, requiring the pilot to take over control.

b. Longitudinal Control. The control law for longitudinal control is not changed. The only major change with respect to the NL, when considering safety, is the loss of the angle-of-attack and pitch protections. This includes the buffer zone described before, as well as the protection against excessive control inputs. Load factor protection is present equal to the NL.

Too large angle-of-attack angles can lead to an aircraft stall and pilots are trained to avoid this event in all circumstances. Most of the time the aircraft flies in the NL, and the aircraft simply cannot stall. But, in the very rare situation that the NL is deactivated and the degraded control laws become active, the angle-of-attack protection is lost. Pilots may fail to notice this control law degradation, and the corresponding loss of protection, which could lead to a stall. This possibly catastrophic event will be taken into consideration in our haptic interface design.

To assist the pilot in this control law, a region with low-speed stability is introduced by Airbus. Dependent on the configuration, 5–10 kt above the stall warning speed V_{SW}, a nose-down signal is introduced. Additionally, an aural "STALL" warning is added with, according to the Airbus documentation, "appropriate margin from stall." Furthermore, bank angle compensation is added to maintain a constant angle of attack.

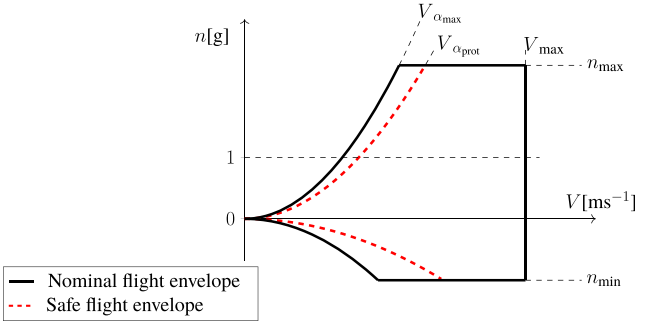

Fig. 6 Flight envelope with A320 longitudinal flight envelope protection limits indicated.

The high-speed stability from the NL remains, yet the pilot is now able to overrule the imposed nose-up command. Autopilot disconnection occurs when the velocity exceeds $V_{\max}$; at $V_{\max} + 4$, an aural "OVERSPEED" warning is present.

3. Alternate Control Law Without Reduced Velocity Protections

In some cases (for example, when all three air data reference units fail), the control laws further degrade and have even less protections. Both lateral and longitudinal control laws remain equal to the AL with the protections, except that the low- and high-speed stabilities are lost. The load factor limitation does remain available for the pilot.

4. Direct Law

When all three inertial reference units fail, the RAs fail when the landing gear is down, or when flaps are selected while the LGCIUs disagree, the control law is reverted even more to the direct law. In this law, control surface deflections become equal to sidestick inputs.

a. Lateral Control. Although direct stick to roll is low-level control, the FCC still aids the pilot, inputting the right magnitude of inputs by scaling the control gains based on the configuration. Yaw damping and turn coordination are lost in this case, as is the maximum bank angle.

b. Longitudinal Control. Stick-to-pitch direct control is aided by scaling the control gains, depending on the center of gravity of the aircraft. In this control law, no protections are active and the pilot can therefore bring the aircraft outside the flight envelope limits.

5. Mechanical Backup

When a complete loss of electrical power is detected, the sidestick is unusable due to the transducers used in the design. Therefore, a mechanical backup is available, which is a very basic and crude control.

a. Lateral Control. Lateral control is achieved solely by operating the rudder pedals, without any direct bank control. Rolling is achieved due to the coupling of yaw and roll but, because this is a slow response, Airbus indicates in the chapter titled "Operational Philosophy—020 Flight Controls" of Ref. [28] to "Gently apply an input and wait for the response." Care should be taken to not exaggerate the input as to not over-control the aircraft.

b. Longitudinal Control. The mechanical backup for the pitch control is made by manually trimming the horizontal stabilizer. Again, this provides a slow control method and should be executed with caution.

Now that the basic flight dynamics are discussed, and the Airbus flight control philosophy summarized, we can move to the design of our haptic interface. That is, how can we use haptics to assist pilots in maintaining situation awareness of the state of the aircraft and the automation, especially in high workload situations when the aircraft operates close to the flight envelope limits?

III. Haptic Display Design

This section describes the haptic display that is used to show the flight envelope boundaries to the pilot. First, the definition of haptic feedback for this research is shown, followed by the goal of the support system. Next, the information is used to elaborate on how and when haptic feedback is provided in the current design. Note that the values for all tuning parameters introduced in the following are summarized in Table 3.

A. Haptic Feedback Definitions

Haptic feedback can be considered as a process that deliberately changes the feel of the control device. This research focuses on changing the haptic profile, i.e., the relation between the deflection of the control device δ and the amount of force required to do so F. A default profile for many sticks (and other control manipulators such as rudder pedals) is a piecewise linear relation, as shown in Fig. 7. Here, δ_{np} is the position of the control device when no force is applied, which is referred to as the neutral point. The location of the breakout zone is given by δ_{br}, where the stick has a spring coefficient k_{br}. The breakout zone is included to haptically show pilots where the "zero stick deflection" position lies. Outside this zone, k^+ and k^- are the spring coefficients for, respectively, positive and negative control device deflections. The default case for this design, as for the Airbus sidestick, is a symmetric profile using a nominal stiffness k_{nom} for positive and negative deflections until a maximum deflection $\delta_{\max}$. Deviations from this default haptic profile can be used to provide the pilot with feedback through the control device. Although not considered here, haptic feedback can also be considered by changing the dynamic properties of the control device such as the natural frequency, the damping coefficient, the static friction (force required to move from a standstill), the dynamic friction (friction due to movement), or other nonlinear phenomena [3].

Table 3 Summary of design parameters for control device and haptic settings

Parameter	Value
K_α	3
K_n	2
$K_{V_{\max}}$	2
k_{nom}	1 N/ deg
$\delta_{\max}$	18 deg
k_{pr}	50 N/ deg
δ_{pr}	0.05 deg
$\tau_{\text{overspeed}}$	15

The literature shows different ways of changing the haptic profile: in the automotive field, there is a strong focus on using a forcing function that can be used as both a warning signal [29,30] or as a guidance force [20,21]. Aerospace applications show examples that add a soft stop (a local step in the amount of force required), a hardstop (a change in maximum deflection) [5], forcing functions [31], changes in the stick neutral position [12], and changes in nominal stick stiffness [32,33]. An example of haptic feedback in the current Airbus A320 flight deck is the detent present on the thrust levers: the controls "click" in the important thrust positions (such as maximum thrust, or the take-off/go-around setting) and require a threshold force to move away from this position.

B. Goal of Support System

We aim to use haptic cues to provide pilots with information on whether the aircraft approaches the limits of the FEP: increase situation awareness. In Sec II.B, we discussed how moving the

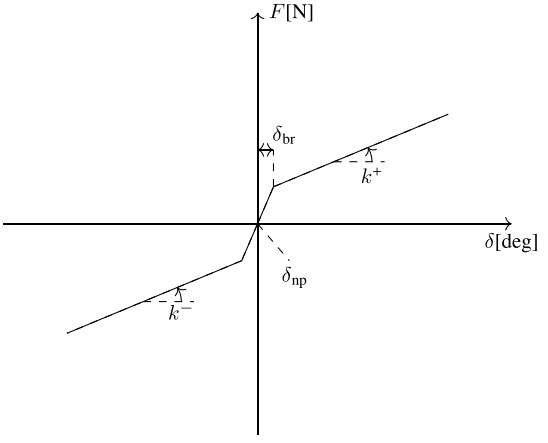

Fig. 7 Nominal control device profile: required force exerted F versus stick deflection δ.

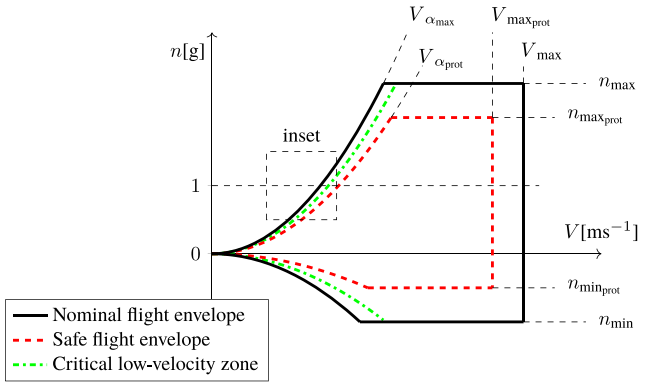

Fig. 8 Flight envelope: load factor n versus velocity V, with inset for Fig. 11.

aircraft outside the SFE, shown in Fig. 8, can lead to changes in the control law. For instance, in the NL, when approaching the maximum angle of attack, the control laws change from C^* to α-position control. So, in principle, the fact that the control law is active does provide some information on the proximity to the boundaries of the FE. Nevertheless, pilots must infer this from the changing aircraft reaction to control inputs or from the velocity indication on the PFD when flying in the NL. To present this more clearly, the haptic support system will include the Airbus protection features expressed with haptic cues. In addition, we will explore how potential mitigation control strategies can be suggested by the haptics, e.g., by making clear what control actions are desired or undesired. The following haptic cues are added and will be discussed in detail in the indicated subsections: 1) a square pulse displaying the transition from inside to outside the SFE, i.e., crossing the red dashed line indicating the SFE in Fig. 8 (Sec. III.D); 2) change in spring coefficient for positive or negative positions relative to the distance from the SFE to the limit, i.e., the distance between the red dashed and the black lines in Fig. 8 (Sec. III.E); 3) changing the neutral point to indicate the automatic control input by the FCC in case of overspeed, i.e., right of the high-speed protection line in Fig. 8 (Sec. III.C); 4) changing the neutral point to indicate a neutral stick position is not sufficient for low velocities near the location of the inset on Fig. 8 (Sec. III.C); and 5) a stick shaker at critical low velocity, i.e., left of the green dashed–dotted line in Fig. 8 (Sec. III.D).

The result on the system architecture is a dependency of the control device properties on the aircraft states and the FEP through the haptic feedback law (HFL), shown on Fig. 9. Note that the HFL is not dependent on the current control device state: the haptic display shows when limits are near, it does not show the control device position where these limits become near. Information on the limits is assumed to be calculated by an external model and is therefore not discussed in this paper. For this research project, a proprietary Airbus A320 model created by the DLR, German Aerospace Center has been made available. More information on the control laws, the flight envelope, and the corresponding protections can be found in Refs. [34,35].

This paper discusses only longitudinal haptic feedback. Furthermore, it is assumed that the pilot is flying with hands on the controls, which is verified in conversations with pilots to be a common airline procedure below an altitude of 10,000 ft and in emergency situations. Additionally, Airbus specifies three phases in flight with different control modes: on the ground, during flare, and in flight [24]. In this research, only "flight mode" is considered. The transitioning modes during flare and on the ground, as well as lateral haptic feedback, are left to a next iteration.

Note that the FE used for the design of the haptic display presented in Fig. 8 has three differences with respect to the FE for Airbus control laws shown in Fig. 6. First, we decreased the upper aircraft velocity limit in the SFE, and we provide a buffer of 20 kt ($V_{max_{prot}} = V_{max} - 20$). Second, to complete the buffer zone toward the hard flight limits, we added a buffer on the load factor of $0.5g$. Third, we implemented a critical low-velocity zone, which will be communicated through the use of forcing functions.

In normal operations, the aircraft is operated within the SFE in the normal control law. In the case of abnormal situations, as discussed in Sec. II.B, the aircraft can revert to an alternate control law in which fewer protections are active and the pilot has more control to move outside the FE. In the current stage of our project, the haptic display is designed such that, in both cases (NL and AL), the haptic settings are identical. The full haptic display can still be applied in the AL because the intensities of the cues will be chosen such that pilots can always overrule the haptic signals: they have the final authority of the side-stick. Hence, in both conditions, in case the aircraft is maneuvered outside the SFE, the haptic cues are designed such that they should support the pilot in identifying the situation, and deciding on an effective mitigation strategy, to keep the aircraft safe.

The remainder of this section elaborates more on how and when the haptic cues are provided.

C. Change the Position of the Neutral Point

The position of the neutral point can be changed through manipulating the value of δ_{np}. If applied, the information provided by the haptic display is directly proportional to a required control command and, in principle, the pilot can "just follow the position." Previous research showed that using such an approach increased tracking performance while reducing the physical effort [31]. If the pilot does not agree, however, (s)he can choose to override the cue and keep the stick position fixed by actively counteracting, using co-contraction of the muscles [36]. Nevertheless, the shift in neutral position gives a clear message to the pilot on what (s)he should do. The effect of this change in neutral position on the profile can be seen in Fig. 10 by the shift of the entire graph to the right.

In the Airbus philosophy, a zero stick deflection gives a commanded load factor of one. This is a safe and desired load factor for most of the flight; but, in some cases, a different load factor is needed to return to the SFE. To indicate this, the neutral point can be altered. Looking at the FE in Fig. 8, two such regions can be identified: 1) in case of overspeed, when an active pull-up is required; and 2) at high load factors for low velocities because the maximum safe load factor is below one. The next sections therefore investigate this required load factor n_{req} for both situations, respectively, followed by the translation of the required load factor to the required change in stick neutral position.

1. *Overspeed*

When an overspeed occurs, the speed has to be reduced actively by the pilot by either reducing the throttle or by pitching up such that

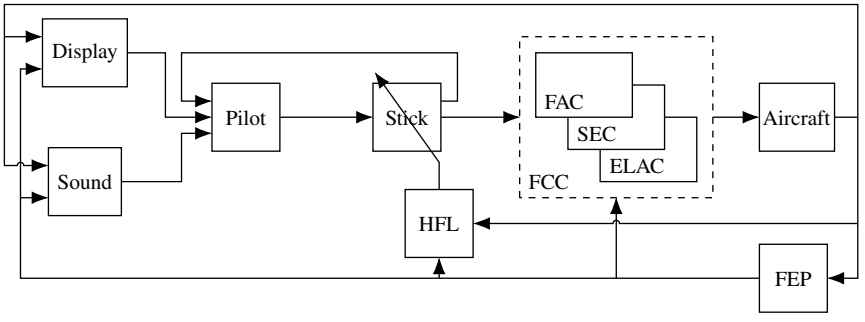

Fig. 9 Block diagram representing the Airbus control loop combined with the haptic feedback law.

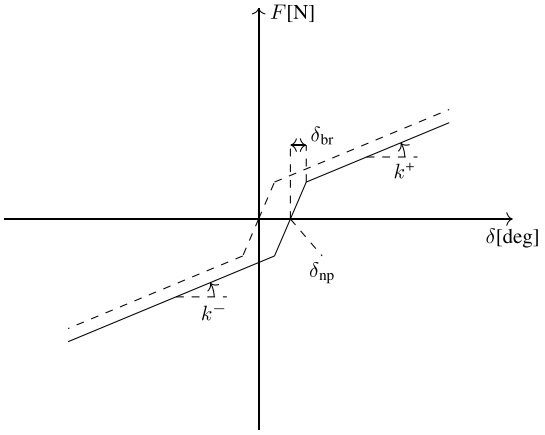

Fig. 10 Haptic profile with a positive shift in the neutral point position.

kinetic energy is exchanged for potential energy. In the current state, the Airbus control law will implement a forced nose-up command (see Sec. II.B), which could be translated to a change in the neutral point. Nevertheless, the actual implementation of this signal is not known for this research and is approximated as described in the following. The main reason for this cue is to inform the pilot that maintaining the stick at zero deflection does not solve the FE violation, and action needs to be taken. Note that, here, our research deviates from the A320 FEP: the nose-up command is not activated when crossing $V_{\max}$; it is already activated when crossing $V_{\max_{\text{prot}}}$.

For this research, the nose-up command, and therefore the magnitude of the neutral point shift, is governed by the change in load factor required to bring the positive acceleration to zero. It is determined by starting from the longitudinal equations of motion [23], where we assume engine thrust to be parallel to the aircraft body:

$$T\cos(\alpha) - D - W\sin(\gamma) = m\frac{\mathrm{d}V}{\mathrm{d}t} \tag{2}$$

From all variables in this equation, the pilot can manipulate the aircraft flight path γ through moving the stick. Here, the neutral point is shifted to obtain a flight path angle such that there is no positive acceleration: $(\mathrm{d}V/\mathrm{d}t) = 0$. Because the aircraft is accelerating, the left part of Eq. (2) is not zero and can be rewritten to obtain a steady flight path:

$$\gamma_{\text{steady}} = \arcsin\left(\frac{T\cos(\alpha) - D}{W}\right) \tag{3}$$

Thrust and drag cannot be measured directly; their effects can be measured through accelerometers, mounted on the aircraft body, which therefore must be rotated to the velocity reference frame:

$$\begin{aligned} T\cos(\alpha) - D = ma_{x_a} = m(a_{x_b}\cos(\beta)\cos(\alpha) + a_{y_a}\sin(\beta) \\ + a_{z_a}\cos(\beta)\sin(\alpha)) \end{aligned} \tag{4}$$

Combining Eq. (3) with Eq. (4) then yields the required change in flight path angle for zero acceleration ($\gamma_{\text{steady}} - \gamma$), all expressed in measured quantities.

As discussed, the sidestick gives load factor commands for high velocities; therefore, a relation between the change in the flight path angle and the load factor is also required. The load factor is governed by the time derivative of the flight path angle; therefore, a tuning factor $\tau_{\text{overspeed}}$ is chosen, which is a measure of the recovery speed:

$$n_{\text{req}} = \frac{V}{g}\tan(\gamma) = \frac{V}{g}\cdot\tan\left(\frac{\gamma_{\text{steady}} - \gamma}{\tau_{\text{overspeed}}}\right) \tag{5}$$

2. G-Loading for Low Velocities

As mentioned before, the stick neutral position commands a load factor of one. In case the aircraft velocity becomes too low (that is, too far to the left in Fig. 8, with a zoomed-in view shown by Fig. 11), returning to a load factor of "one" is not sufficient to re-enter the safe flight envelope, and the pilot has to be informed that action is required.

This is done by shifting the stick neutral point. The prerequisites for this cue are that the current safe load factor is below one and the current load factor (the green circle in Fig. 11) is above the safe load factor. Note that the current load factor is measured by sensors, and it is assumed that the aircraft (model) calculates the safe load factor. The required load factor to return to the SFE is therefore the safe load factor itself $n_{\max_{\text{prot}}}$.

3. Change in Neutral Point Implementation

For the two cases discussed earlier, a required load factor is calculated, which needs to be shown to the pilot using a change in stick neutral deflection. Because zero stick deflection indicates a required load factor of one, the required shift in the neutral point $\Delta\delta_{\text{req}}$ given a required load factor n_{req} can be determined using

$$\Delta\delta_{\text{req}} = \frac{\delta_{\max}}{n_{\max} - 1}(n_{\text{req}} - n) \tag{6}$$

In case this required change in neutral point is implemented immediately, abrupt changes in the control feel can be observed. The change in neutral point would then be perceived more as an "alert" rather than a guidance cue. Therefore, the required change in the neutral point is ramped in linearly using an iterative formula that can be easily implemented in software. With the previous neutral position $\delta_{\text{np}_{\text{prev}}}$, the time difference with the previous step Δt, and the rate δ, the current neutral position δ_{np} is calculated using

$$\delta_{\text{np}} = \min(\Delta\delta_{\text{req}}, \delta_{\text{np}_{\text{prev}}} + \Delta t\delta) \tag{7}$$

D. Add a Forcing Function to the Device

When a forcing function is added to the control device, the whole force/position profile is shifted vertically up or down. Depending on the magnitude of the cue, and whether the pilot is holding the stick or not, it can change the control device deflection, as shown in the illustrative example in Fig. 12a. In our design, we intend to use this cue mainly to alert or warn the pilot, and not to impose a required control input. Hence, the forcing function should be of a small period, or a small amplitude. The effect is therefore short and not predefined in terms of deflection: the effect can be difficult to grasp in one snapshot of a haptic profile. As such, the time trace of the forcing function is visualized by an added graph as shown in Fig. 12b, where zero time is current, and times to the right represent past times. A pragmatic approach is used to evaluate whether the cue complies

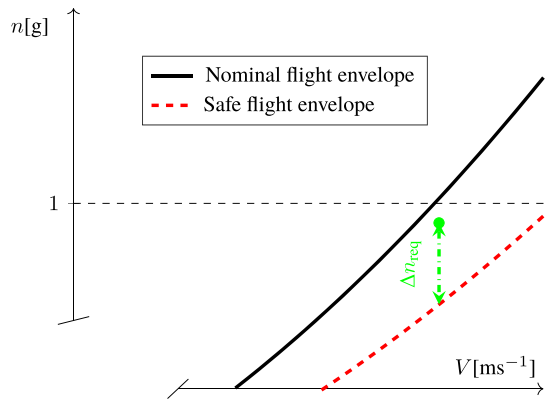

Fig. 11 Amount of load factor change required when flying at low velocities, with inset from Fig. 8.

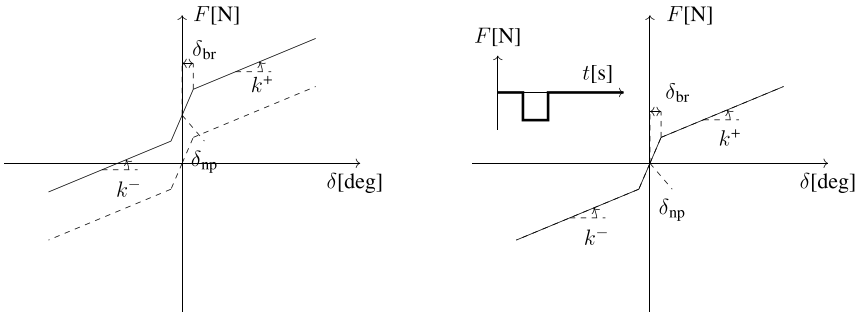

a) Control device shift due to a negative forcing function **b) Added negative (pull) pulse**

Fig. 12 Haptic profiles showing the addition of a forcing function.

with the assumption of a small period or amplitude. In the current design, two forcing functions are used: a discrete cue to communicate the exit of the SFE, and a stick shaker to alert for low velocities.

Note that the addition of a forcing function and a pure change of neutral point both result in a change of position of the control device. Nevertheless, their driving principle is different: a forcing function does not have a predefined effect on the control position. The effect depends on the position of the control device in the haptic profile and the pilot's arm stiffness. In contrast, a pure neutral point shift results in one desired control input to guide a pilot through a maneuver.

1. Discrete Cue

Discrete cues are limited in time and can have a wide variety of shapes, ranging from a square block signal to a noise input. They can be a useful tool to warn the pilot of entering a certain region while not giving a constant signal. The intent of this cue can be compared to a soft stop: an indication of entering a region where caution is required. For example, a soft stop can indicate a position where the maximum engine limits are exceeded [13,37]. In contrast, a forcing function is added to the controls when the (protection) limit is exceeded. The forcing function is chosen in the design because it does not have a dependency on the state of the control device, as do all cues used in the design.

One region that can be entered, with or without the intention of the pilot, is the protected region close to the edge of the FE, shown in Fig. 8 by the dashed line, corresponding to the buffers created on α, n, and V. An example where entering this zone can go unnoticed by the pilot is when he/she is busy scanning the instruments or involved in other tasks. Therefore, to provide a clear transition cue when exceeding the SFE, a warning cue in the form of a square pulse signal (width of 0.1 s and magnitude of 10 N, shown in Fig. 13a) is given. This shape and intensity of the forcing function were chosen based on a preliminary test with a single test pilot; future research is needed for the further definition of this shape. By adding this cue, the pilot is triggered about the SFE departure and the attention is drawn to the event.

The direction of the cue should indicate the direction of the "correct action" for the pilot to perform if (s)he intends to solve the limit violation. For this reason, a stick forward cue ("pitch-down" indication) is given for extreme positive load factors, high angles of attack for positive load factors, and low-velocity violations. A stick backward cue ("pitch-up" indication) is given when crossing all other boundaries.

2. Stick Shaker

A periodic cue is a signal that repeats itself in time, and it can be used as a persistent way to alert pilots of an imminent critical state.

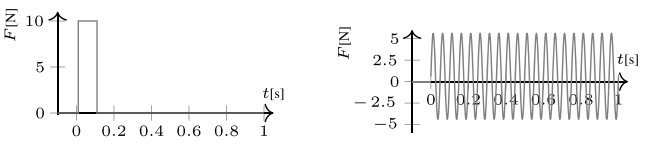

a) Stick push function **b) Stick shaker**

Fig. 13 Continuous forcing functions used.

An example is the motor priming used by Navarro et al. [29] to warn drivers of a lane departure. Analogous to this event, in aerospace, exceeding the maximum angle of attack should be avoided at all times. Hence, to bring extra attention to the proximity to stall, a second forcing function is added: a stick shaker following a sinusoidal forcing function with a frequency of 20 Hz and a 5 N amplitude, shown in Fig. 13b. The frequency and amplitude are tuned to match the stick shaker present in other aircraft (such as Boeing [10]), and they were initially designed to represent the aerodynamic buffeting on the control surfaces.

The stick shaker is activated when the aircraft velocity drops below half of the protected range hence, $(V_{\alpha_{\max}} - V_{\alpha_{\text{prot}}})/2$. In terms of the flight envelope, this means that, close to the left-hand limits of the FE (indicated in Fig. 8 with a dashed–dotted green line), the stick shaker activates. This cue is additional to the existing flight envelope protection as described in Sec. II.B; yet, it is intended to clearly indicate to pilots that the aircraft is moving closer to the lower velocity limit.

E. Change in Spring Coefficient

Previous research increased the spring stiffness to indicate that continued control inputs would result in a hazard, effectively reducing the occurrences of imminent pilot-induced oscillation [32,33], signal a lagging adaptive controller [38], or indicate a helicopter main rotor setting below the limit [37]. In our design, a continued control input results in a hazard when it brings the aircraft closer to the limit. Looking at the FE, it is not just any input that poses a hazard; it is one direction of input that worsens the situation. For example, when the aircraft is close to an overspeed condition, pushing the stick results in a state closer to the actual overspeed, and pulling on the controls is a possible mitigation strategy. Therefore, to show the undesired input, a continuous single-sided spring cue is used, resulting in a haptic profile as shown in Fig. 14c. In this figure, the positive (push) deflection requires more force, indicating an unwanted input as in the preceding examples; a negative (pull) deflection is easier to obtain because the spring stiffness is equal to the nominal value. Note that a change in spring coefficient is only noticeable to pilots when they move the stick away from the neutral point, hence when the pilot is actively controlling. This haptic cue does not necessarily change the control input itself.

Similar to the further spring coefficient increase when the adaptive controller increases lags [38], increasing the spring coefficient can additionally be used to communicate the magnitude of the SFE excursion. As such, starting at the edge of the SFE (the red dashed line in Fig. 8), and up to the edge of the nominal FE (the solid black line in Fig. 8), the stiffness is increased. For the load factor, the velocity, and the angle of attack, we use ν as generic symbol; the default stiffness is multiplied with a factor K_k determined by the gain K_ν and the severity of the violation:

$$K_k = \begin{cases} 1 & \text{if } \nu < \nu_{\text{prot}} \\ 1 + K_\nu & \text{if } \nu > \nu_{\text{nom}} \\ 1 + K_\nu \frac{\nu - \nu_{\text{prot}}}{\nu_{\text{nom}} - \nu_{\text{prot}}} & \text{else} \end{cases} \tag{8}$$

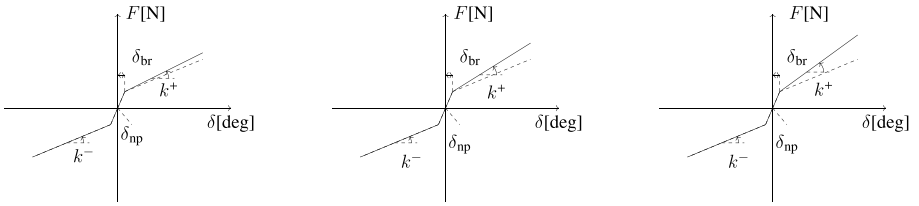

a) Increased k^+ for severity of 0.2 b) Increased k^+ for severity of 0.5 c) Increased k^+ for severity of 1.0

Fig. 14 Haptic profiles showing progressively increasing positive spring stiffness k.

The severity is defined as the ratio of the violation of the SFE ($\nu - \nu_{\text{prot}}$, where ν_{prot} is the value at the edge of the SFE) and the distance between the safe and the nominal FEs ($\nu_{\text{nom}} - \nu_{\text{prot}}$, where ν_{nom} is the value at the edge of the nominal FE). To guarantee that the pilot has the final authority of the sidestick, the stiffness does not increase when the state exceeds the nominal FE. The haptic display is defined to trigger on the maximum $\alpha_{\max}$ and protected α_{prot} angles of attack instead of the lower velocity; nevertheless, these variables are related through Eq. (1).

To illustrate the working principle in the overspeed condition mentioned before, Fig. 14 shows three instances where the velocity is outside the SFE. Figure 14a represents a situation where the severity is 0.2: the velocity is slightly over $V_{\max_{\text{prot}}}$. If the situation gradually evolves, an increased velocity results in Fig. 14b, which shows an increased single-sided stiffness with a severity of 0.5. Finally, Fig. 14c shows a condition at or above $V_{\max}$ where the spring stiffness is maximal; hence, severity is one.

The direction of the stiffness cue is inversed from the discrete cue. That is, the stick feels "stiffer" for backward movement in cases of extreme positive load factors, high angles of attack for positive load factors, and low-velocity violations. All other violations of the SFE will lead to increased stiffness for forward movements. As such, the direction of the stiffness cue informs pilots of control actions that will bring the aircraft closer to its limits: the discrete cue informs which action can resolve the current situation.

As the stiffness changes with continuous variables, no sudden changes in stiffness should occur. Nevertheless, if it occurs, a large change in stiffness could be observed by pilots as a forcing function, hence as an alert and not as a continuous guidance cue. Therefore, to guarantee a smooth change in stiffness, the change is ramped in linearly, similar to Eq. (7).

IV. Operational Test Scenarios

Two relevant operational scenarios will be discussed in this section, which were chosen because we expect that our haptic interface can provide pilots intuitive and useful information to deal with these events; both scenarios are based on Ref. [35]. The first example describes a case in which pilots are required to maneuver close to the edges of the flight envelope limits: a windshear. The second example shows how pilots can use the system when the flight envelope is shrinking and the envelope limits approach the current aircraft status, ultimately limiting pilots in their control: icing. For both scenarios, we will discuss the origin of the event, the required (or: desired) actions to be taken by the pilot, and how we expect that the new haptic system supports the pilot in deciding and performing the necessary actions. In addition, Sec. IV.C discusses some possible undesired actions, which can be further investigated in our experimental evaluation.

A. Windshear: Aircraft Operates Close to the Envelope Limits

A windshear is a meteorological phenomenon in which a large cylinder of air suddenly "drops" toward the Earth [39]. When this cylinder plunges on the Earth surface, the air spreads out, as illustrated in Fig. 15, with the numbers in circles corresponding to those used in the following text, as well as the figures that follow. If an aircraft flies through the wind field, the headwind initially causes its airspeed to increase as in point 2. When the pilots do not recognize the windshear and fail to take action, the downwind that follows will push the aircraft toward the ground (points 3 and 4). The next tailwind drastically reduces the velocity (point 5). Near the final stage of the recovery, the aircraft is flying with high throttle settings and almost level flight: a potential problem is an overspeed (point 6). At the end of this event, the pilots hopefully are able to return to normal flight (point 7). All things considered, windshear forms a severe risk to the safety of the flight, especially during takeoff or landing when already close to the ground [40]. Throughout the windshear recovery, it is vital that pilots use all available aircraft performance to climb, irrespective of forward velocity, with one catch: the aircraft should not be stalled.

If this event occurs with the autopilot active, most actions are handled automatically while the pilot maintains a close watch on the autopilot actions. Here, we focus on manual flight control, and the autopilot is assumed to be turned off. The pilots must perform a set of actions, which are put forward by the manufacturer as described in the FCOM [24].

The initial warnings for the pilot of the oncoming event are a visual and an aural warning: a red "WINDSHEAR" message on the PFD and a synthetic voice that announces "windshear" three times. At this point, the FCOM states that the pilots must take the following six actions:

A) Do not change configuration (flaps, slats, gear) until out of the windshear.

B) Set thrust levers at go-around position.

C) Set pitch attitude initially at 17.5 deg.

D) Increase pitch if necessary to minimize loss of height above terrain.

E) Closely monitor flight path and speed.

F) Recover smoothly to normal climb out of shear.

The first step is a straightforward command to make sure that no time is lost before starting the recovery. Next, one must assure that maximum energy is available (step B), followed by an initial pitch attitude to start increasing altitude (step C). Then, steps D and E are crucial to the safety of the aircraft: here, we see a tradeoff between, on the one hand, reducing altitude loss and, on the other hand, maintaining sufficient airspeed. In case of an extreme windshear, this recovery procedure might require pilots to move dangerously close to the limits of the flight envelope, namely, at very low velocities to use all available energy to climb out of the shear. The final step (step F)

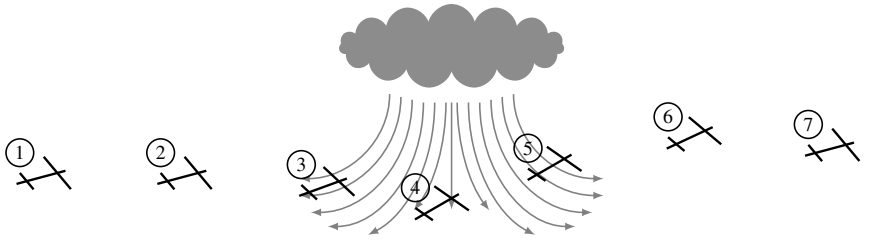

Fig. 15 Weather structure during windshear.

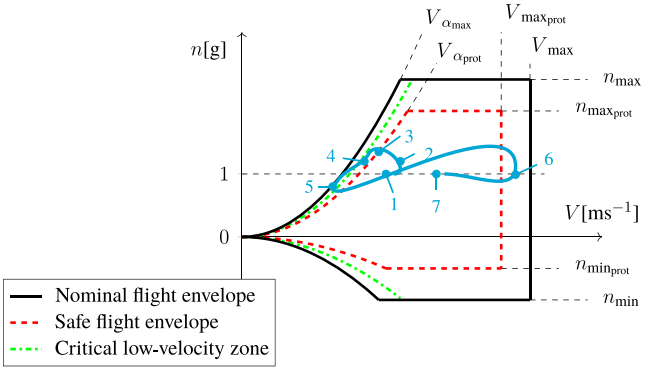

Fig. 16 Trajectory through the flight envelope during windshear recovery, with frames indicated in Fig. 15.

assures that, when clear of the dangerous winds (yet still with high throttle settings), the aircraft velocity does not exceed the upper limit.

Throughout the procedure, pilots are likely to work under high workload levels and could develop a mental state of "cognitive tunneling," heavily monitoring the loss of height [41]. A support to improve the attention division of the pilot is of crucial importance, and we show in the following that our haptic interface can enable this.

The trajectory in the FE of the seven selected timeframes is shown in Fig. 16. For each frame, the leftmost column of Fig. 17 shows the aircraft FEs, with the current aircraft state shown using a circle. The center column shows the corresponding PFDs, with the velocity (left), altitude (right), and attitude (center). The rightmost column of Fig. 17 shows the haptic profile. These frames are used here to show how the haptic interface is working during operations. For example, the first of these frames is the starting point when the windshear warning becomes active; the corresponding FE, PFD, and haptic profile can be seen in, respectively, Figs. 17a–17c.

After the warning is given, our haptic interface is expected to help in the following steps (corresponding to the list of actions stipulated by the FCOM):

C) The pilot must pitch-up the aircraft, and this increases the load factor somewhat (frame 2). If this maneuver is executed too fast, the pilot is informed of the g-loading limit through the load factor protection cues.

D) During this step, as much energy as possible should be used to climb; and the haptic system is expected to help pilots to operate at or close to the flight envelope limits. The initial cue of approaching limits is the discrete cue, corresponding to frame 3 in Fig. 17.

E) As the pilot has to divide attention over two elements of the PFD (the velocity and altitude indicators) and possible cognitive tunneling may develop on the vertical speed, the haptic system is expected to serve as a velocity monitoring aid. This can be achieved by both the continuous spring cue and the change in neutral position for low velocities, as illustrated in frames 4 and 5 in Fig. 17, respectively. Additionally, we expect pilots to use the stick shaker as a possible control aid to "ride the stick shaker," adjusting the input such that the stick shaker remains on the verge of activation.

F) When approaching the upper limit on velocity, the high-velocity cues alert the pilot of an imminent limit violation with an extra control aid by which the pilot can follow the stick backward position, shown in frame 6 in Fig. 17.

In general, for each of the steps, the discrete haptic pulse cue (frame 3) is expected to first alert the pilot that a FE limit is approaching, and then the continuous spring cue (frame 4) follows to clearly communicate the distance left to the ultimate flight envelope boundaries.

B. Icing: Limits Move Toward the Aircraft

The second scenario we will use to evaluate our haptic interface is an extreme form of ice formation on the aircraft wings. Especially when flying through cold humid air, the risk of such an event is severe [42]. The effect of ice formation is a degradation of the aircraft aerodynamic performance, resulting in a reduced lift from the wings and, with that, an increase in the aircraft minimum velocity. Here, it is assumed that the FEP has an updating algorithm, which was presented with icing implementation in Ref. [35]. The decrease in minimal velocity highlights the main difference with the previous scenario: in this case, the flight envelope shrinks, the FE limits "approach the pilot," and (s)he must identify this situation properly and act on it.

An example case of such an event is during a manual instrument landing in which the landing is performed in the clouds. If extreme ice accumulation is present, or when the deicing system is not working properly, the ice formation is an inherently slow yet detrimental process. It is very likely that, for considerable time, pilots may not be aware of the deteriorating aerodynamic properties.

In principle, pilots can notice the degradation of the aerodynamic properties due to icing through two clues. First, the increase in drag requires a higher throttle setting; and second, the decrease of lift requires a higher angle of attack.

Especially when the pilot is flying with the autothrust active, the increase in throttle setting can be more difficult to notice and, as Airbus aircraft by default do not have an angle-of-attack indicator, pilots might be unaware of the creeping danger. Nevertheless, the haptic feedback system uses information on the angle-of-attack sensor, and therefore the pilot will get new information without adding another element on the, already comprehensive, visual display.

To illustrate how the state is developing and how the haptic feedback is supplying flight envelope information, Fig. 18 shows five frames of an icing event in which the FE is shrinking. The leftmost column shows the aircraft FEs, with the current aircraft state shown using a circle. The center column shows the corresponding PFDs, with the velocity (left), altitude (right), and attitude (center). The rightmost column shows the haptic profile. Starting from the nominal condition in frame 1, icing forms and the minimal velocity is increasing as stated before. If the pilots do not react to this, the first signal from the haptic display is the discrete cue when exiting the SFE as in frame 2. At this point, the pilots should become aware that something is going on. Additionally, they have received the correct action by the direction of the cue: reduce the angle of attack. When the pilot keeps controlling in the low-velocity region, the increased spring coefficient for negative deflections (pull) in frame 3 indicates that pulling should be executed with caution. Crossing the stick shaker activation threshold gives a clear cue that a stall is imminent, shown by frame 4. Finally, if the pilot still does not react, the state in frame 5 is at the upper angle-of-attack limit where the stiffness is maximum, the stick shaker is active, and the neutral point shift is most observable: all cues that inform the pilot of the proximity of the FE to the state.

C. Possible Undesired Actions

The previous sections discussed the intended use of the proposed haptic feedback system. We now look at possible undesired actions, which are discussed using the concepts of misuse, disuse, and abuse as proposed by Parasuraman and Riley [43].

Misuse is the use of the automation for an unintended goal, typically due to overreliance on the system. In the case of the haptic feedback system, overreliance can result in a lack of scanning the instruments: the pilot might expect the haptic feedback to signal an approaching limit and focus on other tasks besides the primary flight duty. As the feedback system is reliant on sensor measurements, if these sensors fail, the haptic system might not trigger, whereas a scan of the instruments might show the erroneous measurement. In an evaluation experiment, the presence of overreliance on the haptic feedback system might give different results in the scenarios discussed previously: in the case of windshear, the pilot is actively maneuvering the aircraft closer to the limits and more likely to be aware of a closing limit; in the case of icing, the limits move to the current state; and in the case of overreliance, this event can surprise the pilots.

Disuse is deliberately not using the automation available, which is commonly caused by a distrust in the system due to a significant false alarm rate. Looking at the haptic feedback system while assuming that it functions as intended (no false positives), pilots might still consider the haptic feedback as false when it would be perceived as out of tune with respect to the magnitude of the flight envelope protection zones. For instance, the haptic feedback might signal a

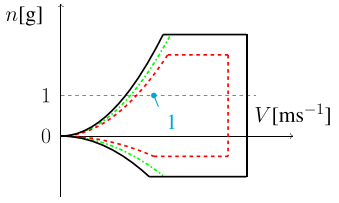

a) FE for frame 1

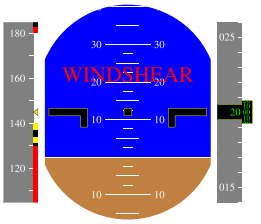

b) PFD for frame 1

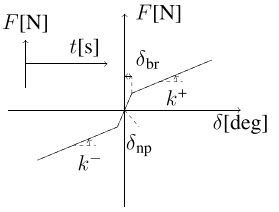

c) Haptic profile for frame 1

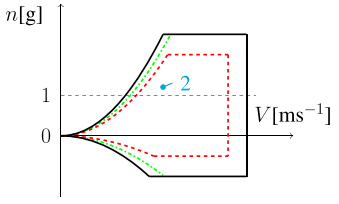

d) FE for frame 2

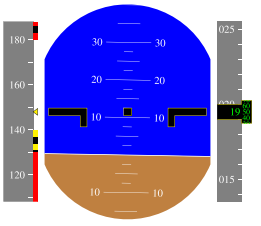

e) PFD for frame 2

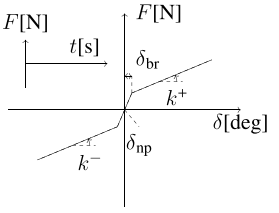

f) Haptic profile for frame 2

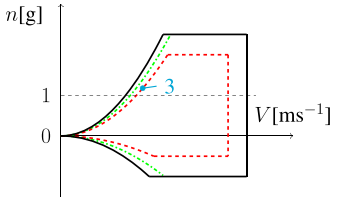

g) FE for frame 3

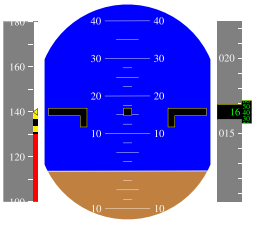

h) PFD for frame 3

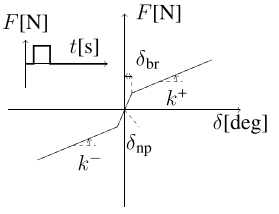

i) Haptic profile for frame 3

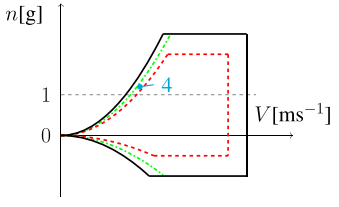

j) FE for frame 4

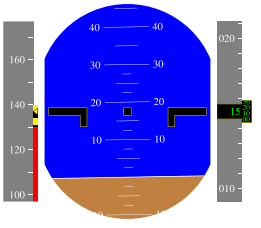

k) PFD for frame 4

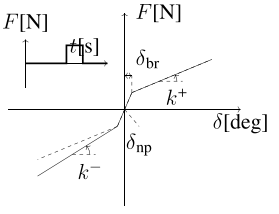

l) Haptic profile for frame 4

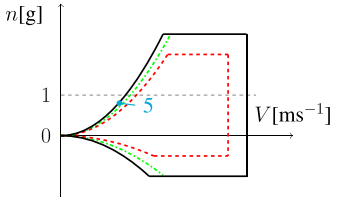

m) FE for frame 5

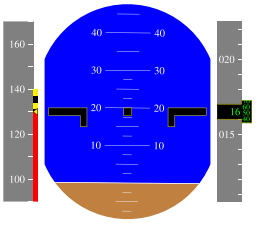

n) PFD for frame 5

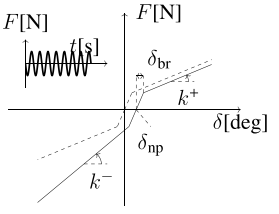

o) Haptic profile for frame 5

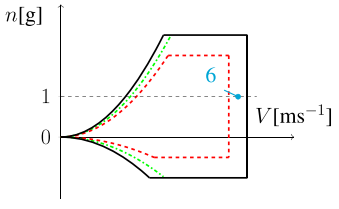

p) FE for frame 6

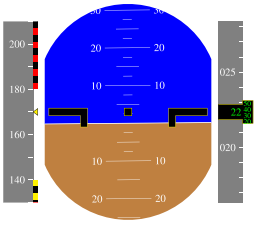

q) PFD for frame 6

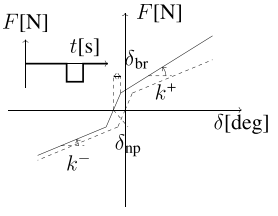

r) Haptic profile for frame 6

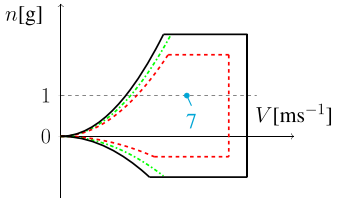

s) FE for frame 7

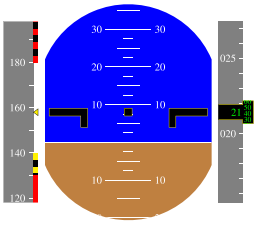

t) PFD for Frame 7

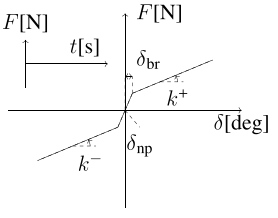

u) Haptic profile for frame 7

Fig. 17 FEs, PFDs, and haptic profiles for the windshear recovery according to the frames from Fig. 15.

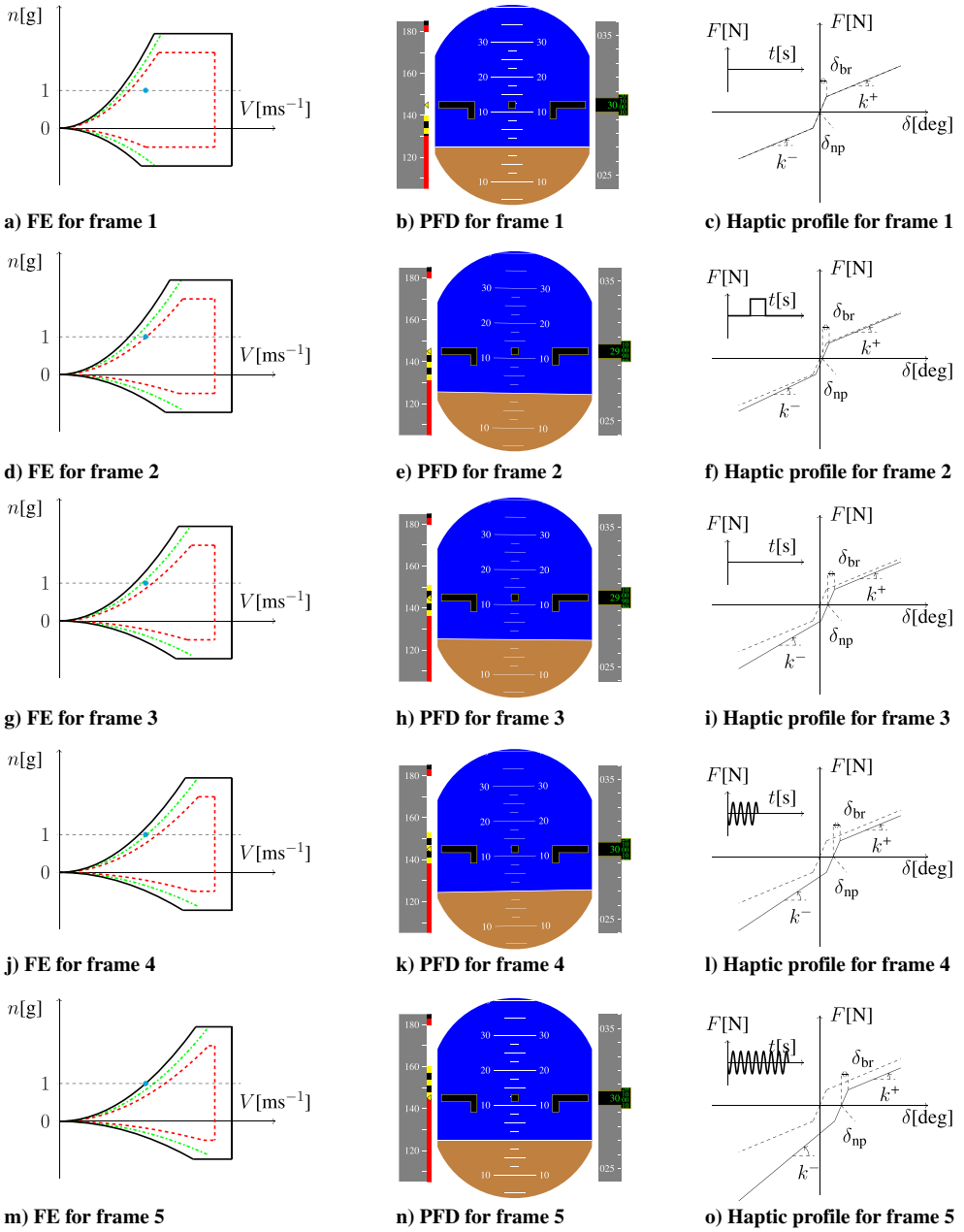

a) FE for frame 1 b) PFD for frame 1 c) Haptic profile for frame 1

d) FE for frame 2 e) PFD for frame 2 f) Haptic profile for frame 2

g) FE for frame 3 h) PFD for frame 3 i) Haptic profile for frame 3

j) FE for frame 4 k) PFD for frame 4 l) Haptic profile for frame 4

m) FE for frame 5 n) PFD for frame 5 o) Haptic profile for frame 5

Fig. 18 FEs, PFDs, and haptic profiles for an icing event illustrating shrinking of the FE.

limit as close, whereas the pilot does not experience it as such. In that case, the haptic feedback might be considered as distracting when controlling the airplane; in a worse case, the pilots can feel that they are fighting the haptic feedback system. An evaluation of the system therefore has to check that the workload of the pilots does not increase, and that pilot actions and haptic feedback are in line.

Abuse is the automation of functions by designers without due regard for the consequences for human performance. In the haptic feedback design, part of the design parameters (for example, the magnitude of the discrete cue) is heuristically tuned using one test pilot. Due to this heuristic tuning, the haptic feedback might be experienced by some pilots as intrusive. As such, an evaluation has to investigate whether the current setup does not increase workload, and it allows the pilot to keep performing the nominal mission.

This provides a set of criteria for the haptic display of flight envelope limits: the haptic feedback system should not increase workload and should not hinder the primary pilot tasks. Furthermore, it should be investigated that overreliance is not present, and that pilots are not fighting with the system. Additionally, performance and safety metrics of pilots flying both windshear and icing scenarios should improve. In conclusion, we expect that the new haptic display presented in this paper increases the knowledge of the pilot on the edges of the flight envelope and helps identify abnormal situations. This hypothesis is tested with an experimental evaluation, which will be the subject of another paper.

V. Conclusions

This paper describes the design of a haptic feedback system, i.e., using force feedback through the control device to provide intuitive information on the state of the aircraft relative to the flight envelope protection. The system 1) informs the pilot about an approaching limit using a discrete cue, 2) indicates a non-desired control direction using the spring coefficient, 3) warns the pilot of a dangerously low velocity using a stick shaker, 4) shows a desired control input during an overspeed event by moving the control device, and 5) indicates the required control input at low velocities when a stick neutral position is not sufficient by moving the control device.

References

[1] Harris, D., *Human Factors for Civil Flight Deck Design*, Ashgate Publishing Ltd., Cornwall, England, U.K., 2004, pp. 69–102, 141–155, Chaps. 4, 6.

[2] van Erp, J. B. F., Kyung, K., Kassner, S., Carter, J., Brewster, S., Weber, G., and Andrew, I., "Setting the Standards for Haptic and Tactile Interactions: ISO's Work," *Haptics: Generating and Perceiving Tangible Sensations*, edited by A. M. L. Kappers, J. B. F. van Erp, W. M. Bergmann Tiest, and F. C. T. van der Helm, Springer, Berlin, 2010, pp. 353–358.
https://doi.org/10.1007/978-3-642-14075-4_52

[3] "Ergonomics of Human-System Interaction—Part 910: Framework for Tactile and Haptic Interaction (ISO)," International Organization for Standardization, STD "9241-910:2011," Brussels, July 2011.

[4] Corps, S. G., "Airbus A320 Side Stick and Fly by Wire—An Update," *Proceedings of the Aerospace Technology Conference and Exposition*, SAE International TP 861801, Warrendale, PA, 1986.
https://doi.org/10.4271/861801

[5] Hegg, J. W., Smith, M. P., and Yount, L., "Sidestick Controllers for Advanced Aircraft Cockpits," *Proceedings of the IEEE/AIAA 11th Digital Avionics Systems Conference*, IEEE Publ., Piscataway, NJ, 1992, pp. 491–499.
https://doi.org/10.1109/DASC.1992.282112

[6] Warwick, G., "Active Sidestick Controls Make Commercial Debut," *Aviation Week and Space Technology*, 2015, https://aviationweek.com/aerospace/active-sidestick-controls-make-commercial-debut [accessed 14 Nov. 2017].

[7] "Final Report on the Accident on 1st June 2009 to the Airbus A330-203 Registered F-GZCP Operated by Air France Flight AF 447 Rio de Janeiro - Paris," Bureau d'Enquêtes et d'Analyses pour la Sécurité de l'Aviation Civile, TR f-cp090601en, Le Bourget Cedex, France, June 2009 (in English).

[8] Gibson, J. C., and Hess, R. A., *Stick and Feel System Design*, AGARD, Neuilly-Sur-Seine, France, 1997, pp. 34–36, Chap. 1.4.

[9] Cook, R. H., "An Automatic Stall Prevention Control for Supersonic Fighter Aircraft," *Journal of Aircraft*, Vol. 2, No. 3, 1965, pp. 171–175.
https://doi.org/10.2514/3.43636

[10] "777 Flight Crew Training Manual," The Boeing Company TR FCT 777, Chicago, Illinois, 2008.

[11] Schmidt-Skipiol, F. J. J., and Hecker, P., "Tactile Feedback and Situation Awareness," *15th AIAA Aviation Technology, Integration, and Operations Conference*, AIAA Paper 2015-2905, 2015.
https://doi.org/10.2514/6.2015-2905

[12] Stepanyan, V., Krishnakumar, K., Dorais, G., Reardon, S., Barlow, J., Lampton, A., and Hardy, G., "Loss-of-Control Mitigation via Predictive Cuing," *Journal of Guidance, Control, and Dynamics*, Vol. 40, No. 4, 2017, pp. 831–846.
https://doi.org/10.2514/1.G001731

[13] Whalley, M. S., Hindson, W., Thiers, G., and Rutkowski, M., "A Comparison of Active Sidestick and Conventional Inceptors for Helicopter Flight Envelope Tactile Cueing," *Proceedings of the 56th American Helicopter Society Forum*, AHS, Alexandria, VA, 2000, p. 24, https://ntrs.nasa.gov/search.jsp?R=20000092066 [retrieved 27 July 2018].

[14] Sahasrabudhe, V., Horn, J. F., Sahani, N., Faynberg, A., and Spaulding, R., "Simulation Investigation of a Comprehensive Collective-Axis Tactile Cueing System," *Journal of the American Helicopter Society*, Vol. 51, No. 3, 2006, pp. 215–224.
https://doi.org/10.4050/1.3092883

[15] von Grünhagen, W., Müllhäuser, M., Abildgaard, M., and Lantzsch, R., "Active Inceptors in FHS for Pilot Assistance Systems," *Proceedings of the 36th European Rotorcraft Forum*, Paris, France, 2010, Paper 134, http://doi.org/20.500.11881/935.

[16] Fellah, K., and Huiatni, M., "Tactile Display Design for Flight Envelope Protection and Situational Awareness," *IEEE Transactions on Haptics*, Vol. 12, No. 1, 2019, pp. 87–98.
https://doi.org/10.1109/TOH.2018.2865302

[17] Ackerman, K. A., Talleur, D. A., Carbonari, R. S., Xargay, E., Seefeldt, B. D., Kirlik, A., Hovakimyan, N., and Trujillo, A. C., "Automation Situation Awareness Display for a Flight Envelope Protection System," *Journal of Guidance, Control, and Dynamics*, Vol. 40, No. 4, 2017, pp. 964–980.
https://doi.org/10.2514/1.G000338

[18] de Stigter, S., Mulder, M., and van Paassen, M. M., "Design and Evaluation of a Haptic Flight Director," *Journal of Guidance, Control, and Dynamics*, Vol. 30, No. 1, 2007, pp. 35–46.
https://doi.org/10.2514/1.20593

[19] Smisek, J., Sunil, E., van Paassen, M. M., Abbink, D. A., and Mulder, M., "Neuromuscular-System-Based Tuning of a Haptic Shared Control Interface for UAV Teleoperation," *IEEE Transactions on Human-Machine Systems*, Vol. 47, No. 4, 2017, pp. 449–461.
https://doi.org/10.1109/THMS.6221037

[20] Mulder, M., Pauwelussen, J. J., van Paassen, M. M., Mulder, M., and Abbink, D. A., "Active Deceleration Support in Car Following," *IEEE Transactions on Systems, Man, and Cybernetics Part A:Systems and Humans*, Vol. 40, No. 6, 2010, pp. 1271–1284.
https://doi.org/10.1109/TSMCA.2010.2044998

[21] Petermeijer, S. M., Abbink, D. A., Mulder, M., and De Winter, J. C. F., "The Effect of Haptic Support Systems on Driver Performance: A Literature Survey," *IEEE Transactions on Haptics*, Vol. 8, No. 4, 2015, pp. 467–479.
https://doi.org/10.1109/TOH.2015.2437871

[22] Ellerbroek, J., Rodriguez Martin, M. J. M., Lombaerts, T. J. J., van Paassen, M. M., and Mulder, M., "Design and Evaluation of a Flight Envelope Protection Haptic Feedback System," *IFAC-PapersOnLine*, Vol. 49, No. 19, 2016, pp. 171–176.
https://doi.org/10.1016/j.ifacol.2016.10.481

[23] Ruijgrok, G. J. J., *Elements of Airplane Performance*, 2nd ed., VSSD, Delft, The Netherlands, 2009, pp. 1–23, 51–62, Chaps. 1, 3.

[24] "A319/A320/A321 Flight Crew Operating Manual," Airbus TR 36, 2003.

[25] Chatrenet, D., "Les Qualités de Vol des Avions de Transport Civil à Commandes de Vol Électriques," *Active Control Technology: Applications and Lesson Learned*, AGARD CP-560, Neuilly-Sur-Seine, France, 1995, p. 5.

[26] Favre, C., "Fly-by-Wire for Commercial Aircraft: The Airbus Experience," *International Journal of Control*, Vol. 59, No. 1, 1994, pp. 139–157.
https://doi.org/10.1080/00207179408923072

[27] Niedermeier, D., and Lambregts, A. A., "Fly-by-Wire Augmented Manual Control—Basic Design Considerations," *28th International Congress of the Aeronautical Sciences*, Vol. 100, ICAS, Edinburgh, U.K., 2012, pp. 1–14, http://www.icas.org/ICAS_ARCHIVE/ICAS2012/ [accessed 16 Dec. 2019].

[28] "A318/A319/A320/A321 Flight Crew Training Manual," Tech. Rept., The Airbus Company, 2015.

[29] Navarro, J., Mars, F., Forzy, J.-F., El-Jaafari, M., and Hoc, J.-M., "Objective and Subjective Evaluation of Motor Priming and Warning Systems Applied to Lateral Control Assistance," *Accident Analysis and Prevention*, Vol. 42, No. 3, 2010, pp. 904–912.
https://doi.org/10.1016/j.aap.2009.07.008

[30] Huang, Z., Wu, Y., and Liu, J., "Research on Effects of Pattern, Amplitude and Frequency of Pulse Steering Torque Warnings for Lane Departure," *Transportation Research, Part F*, Vol. 31, May 2015, pp. 67–76.
https://doi.org/10.1016/j.trf.2015.03.008.

[31] Olivari, M., Nieuwenhuizen, F., Bülthoff, H., and Pollini, L., "Pilot Adaptation to Different Classes of Haptic Aids in Tracking Tasks," *Journal of Guidance, Control, and Dynamics*, Vol. 37, No. 6, 2014, pp. 1741–1753.
https://doi.org/10.2514/1.G000534

[32] Jeram, G. J., and Prasad, J. V. R., "Tactile Avoidance Cueing for Pilot Induced Oscillation," *AIAA Atmospheric Flight Mechanics Conference and Exhibit*, AIAA Paper 2003-5311, 2003.
https://doi.org/10.2514/6.2003-5311

[33] Klyde, D. H., and McRuer, D. T., "Smart-Cue and Smart-Gain Concepts Development to Alleviate Loss of Control," *Journal of Guidance, Control, and Dynamics*, Vol. 32, No. 5, 2009, pp. 1409–1417.
https://doi.org/10.2514/1.43156

[34] Lombaerts, T. J. J., and Looye, G. H. N., "Design and Flight Testing of Nonlinear Autoflight Control Laws," *AIAA Guidance, Navigation, and Control Conference*, AIAA Paper 2012-4982, 2012.
https://doi.org/10.2514/6.2012-4982

[35] Lombaerts, T. J. J., Looye, G. H. N., Ellerbroek, J., and Rodriguez Martin, M., "Design and Piloted Simulator Evaluation of Adaptive Safe Flight Envelope Protection Algorithm," *Journal of Guidance, Control, and Dynamics*, Vol. 40, No. 8, 2017, pp. 1902–1924.
https://doi.org/10.2514/1.G002525

[36] Abbink, D. A., and Mulder, M., "Exploring the Dimensions of Haptic Feedback Support in Manual Control," *Journal of Computing and Information Science in Engineering*, Vol. 9, No. 1, 2009, Paper 11006.
https://doi.org/10.1115/1.3072902

[37] Whalley, M. S., and Achache, M., "Joint U.S./France Investigation of Helicopter Flight Envelope Limit Cueing," *Proceedings of the 52nd American Helicopter Society Forum*, AHS, Alexandria, VA, 1996, p. 30.

[38] Klyde, D. H., Richards, N., and Cogan, B., "Mitigating Unfavorable Pilot Interactions with Adaptive Controllers in the Presence of Failures/Damage," *AIAA Atmospheric Flight Mechanics Conference*, AIAA Paper 2011-6538, 2011.
https://doi.org/10.2514/6.2011-6538

[39] "Windshear Training Aid—Volume 1. Overview, Pilot Guide, Training Program," Tech. Rept., Federal Aviation Administration, 1987.

[40] Evans, J. K., "An Examination of Aviation Accidents Associated with Turbulence, Wind Shear and Thunderstorm," NASA CR-2013-217989, 2013, https://ntrs.nasa.gov/search.jsp?R=20130013459 [retrieved 2019].

[41] Wickens, C. D., and Alexander, A. L., "Attentional Tunneling and Task Management in Synthetic Vision Displays," *International Journal of Aviation Psychology*, Vol. 19, No. 2, 2009, pp. 182–199. https://doi.org/10.1080/10508410902766549

[42] *Instrument Flying Handbook (FAA-H-8083-15B)*, U. S. Dept. of Transportation, Federal Aviation Administration, Airman Testing Standards Branch, Oklahoma City, OK, 2012, pp. 13–17, Chap. 4.

[43] Parasuraman, R., and Riley, V., "Humans and Automation: Use, Misuse, Disuse, Abuse," *Human Factors: The Journal of the Human Factors and Ergonomics Society*, Vol. 39, No. 2, 1997, pp. 230–253. https://doi.org/10.1518/001872097778543886